NASA/TM–2014-218182

Selection of Thermal Worst-Case Orbits via Modified Efficient Global Optimization

Timothy M. Moeller and Alan W. Wilhite
Georgia Institute of Technology, Atlanta, Georgia

Kaitlin A. Liles
Langley Research Center, Hampton, Virginia

March 2014

NASA STI Program . . . in Profile

Since its founding, NASA has been dedicated to the advancement of aeronautics and space science. The NASA scientific and technical information (STI) program plays a key part in helping NASA maintain this important role.

The NASA STI program operates under the auspices of the Agency Chief Information Officer. It collects, organizes, provides for archiving, and disseminates NASA's STI. The NASA STI program provides access to the NASA Aeronautics and Space Database and its public interface, the NASA Technical Report Server, thus providing one of the largest collections of aeronautical and space science STI in the world. Results are published in both non-NASA channels and by NASA in the NASA STI Report Series, which includes the following report types:

- TECHNICAL PUBLICATION. Reports of completed research or a major significant phase of research that present the results of NASA Programs and include extensive data or theoretical analysis. Includes compilations of significant scientific and technical data and information deemed to be of continuing reference value. NASA counterpart of peer-reviewed formal professional papers, but having less stringent limitations on manuscript length and extent of graphic presentations.

- TECHNICAL MEMORANDUM. Scientific and technical findings that are preliminary or of specialized interest, e.g., quick release reports, working papers, and bibliographies that contain minimal annotation. Does not contain extensive analysis.

- CONTRACTOR REPORT. Scientific and technical findings by NASA-sponsored contractors and grantees.

- CONFERENCE PUBLICATION. Collected papers from scientific and technical conferences, symposia, seminars, or other meetings sponsored or co-sponsored by NASA.

- SPECIAL PUBLICATION. Scientific, technical, or historical information from NASA programs, projects, and missions, often concerned with subjects having substantial public interest.

- TECHNICAL TRANSLATION. English-language translations of foreign scientific and technical material pertinent to NASA's mission.

Specialized services also include organizing and publishing research results, distributing specialized research announcements and feeds, providing information desk and personal search support, and enabling data exchange services.

For more information about the NASA STI program, see the following:

- Access the NASA STI program home page at *http://www.sti.nasa.gov*

- E-mail your question to help@sti.nasa.gov

- Fax your question to the NASA STI Information Desk at 443-757-5803

- Phone the NASA STI Information Desk at 443-757-5802

- Write to:
   STI Information Desk
   NASA Center for AeroSpace Information
   7115 Standard Drive
   Hanover, MD 21076-1320

Selection of Thermal Worst-Case Orbits via Modified Efficient Global Optimization

Timothy M. Moeller and Alan W. Wilhite
Georgia Institute of Technology, Atlanta, Georgia

Kaitlin A. Liles
Langley Research Center, Hampton, Virginia

March 2014

TABLE OF CONTENTS

LIST OF TABLES

LIST OF FIGURES

Abstract

Efficient Global Optimization (EGO) was used to select orbits with worst-case hot and cold thermal environments for the Stratospheric Aerosol and Gas Experiment (SAGE) III. The SAGE III system thermal model changed substantially since the previous selection of worst-case orbits (which did not use the EGO method), so the selections were revised to ensure the worst cases are being captured. The EGO method consists of first conducting an initial set of parametric runs, generated with a space-filling Design of Experiments (DoE) method, then fitting a surrogate model to the data and searching for points of maximum Expected Improvement (EI) to conduct additional runs. The general EGO method was modified by using a multi-start optimizer to identify multiple new test points at each iteration. This modification facilitates paralell computing and decreases the burden of user interaction when the optimizer code is not integrated with the model. Thermal worst-case orbits for SAGE III were successfully identified and shown by direct comparison to be more severe than those identified in the previous selection. The EGO method is a useful tool for this application and can result in computational savings if the initial Design of Experiments (DoE) is selected appropriately.

Nomenclature

CCD	Charge Coupled Device
CMP	Contamination Monitoring Package
DMP	Disturbance Monitoring Package
DoE	Design of Experiments
EGO	Efficient Global Optimization
EI	Expected Improvement
ELC-4	ExPRESS Logistics Carrier 4
EOTP	Enhanced Orbital Replacement Unit Temporary Platform
ExPA	ExPRESS Pallet Adapter
ExPRESS	Expedite the Processing of Experiments to Space Station
HEU	Hexapod Electronics Unit
HMA	Hexapod Mechanical Assembly
IAM	Interface Adapter Module
ICE	Instrument Control Electronics
IP	Instrument Payload
ISS	International Space Station
LaRC	Langley Research Center
MBS	Mobile Base System
PSO	Particle Swarm Optimization
RVDT	Rotary Variable Differential Transformer
SA	Sensor Assembly
SAGE	Stratospheric Aerosol and Gas Experiment
SQP	Sequential Quadratic Programming

1 Introduction

SAGE III is the fifth in a series of instruments developed for monitoring aerosols and gaseous constituents in the stratosphere and troposphere. SAGE III measures solar occultation, as shown in Figure 1. Lunar occultation is measured in a similar fashion. SAGE III also measures the scattering of solar radiation in the Earth's atmosphere (called limb scattering) as shown in Figure 2. These scientific measurements provide the basis for the analysis of the atmospheric profiles of aerosols, ozone (O_3), nitrogen dioxide (NO_2), water vapor (H_2O), and air density using oxygen (O_2)[1].
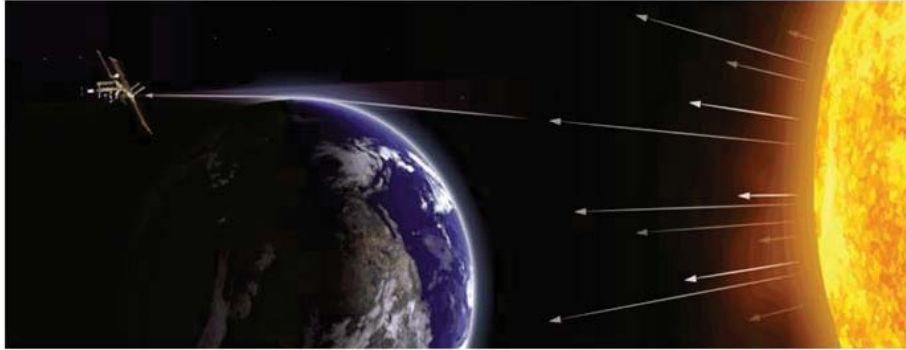
Figure 1: Solar Occultation Measurement[1].

Figure 2: Limb Scattering Technique[1].

The SAGE III Instrument Payload, shown in Figure 3, will be launched to the International Space Station (ISS) in a SpaceX Dragon spacecraft, then transferred on the Enhanced Orbital Replacement Unit Temporary Platform (EOTP) aboard the Mobile Base System (MBS) to its mounting location on the Expedite the Processing of Experiments to Space Station (ExPRESS) Logistics Carrier 4, where it will be mounted for an operational lifetime of 3 years. Many types of thermal analysis are required to validate the payload during transfer and in the final mounted configuration on ISS. More information on the overall thermal modeling approach used for SAGE III is presented by Liles, et al.[1]
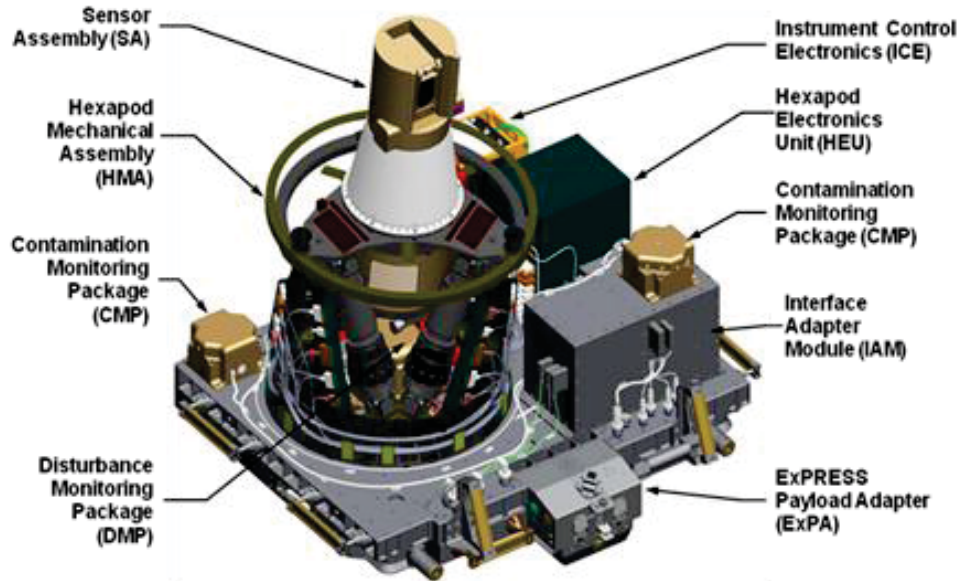
Figure 3: SAGE III Instrument Payload (IP)[1].

This report describes work to revise the SAGE III worst-case thermal environment definitions for the payload in its ISS mounted configuration on ExPRESS Logistics Carrier 4 (ELC-4) and during transfer on EOTP. The selection of orbits with worst-case thermal environments was done once previously, but the thermal model has changed significantly since that time. Therefore, it is necessary to verify that the worst-case orbits are being captured prior to finalizing the pre-flight predictions for SAGE III.

To determine the worst-case beta angle and attitude combinations for hot and cold cases on ELC-4 and EOTP, a method called Efficient Global Optimization[2] (EGO) was used. This method consisted of first conducting an initial set of parametric runs, generated with a space-filling Design of Experiments (DoE) method, then fitting a surrogate model to the data and searching for points of maximum Expected Improvement (EI) to conduct additional runs. The approach that was previously used for selecting the worst-case orbits consisted of simply selecting the most severe cases from a DoE set of parametric runs without selecting additional test points. Since the EGO approach had not previously been tested for this application, the initial DoE runs were selected to be sufficient by themselves to provide the same level of accuracy and confidence as the previous effort to define worst-case environments.

2 Background

SAGE III has developed an analysis approach which incorporates two sets of worst-case environments. One set of environments (referred to as "ISS Extreme") is used to verify that ISS program requirements are met (i.e. that SAGE III does not damage ISS or its payloads) and one set of environments is used to assure SAGE III mission success. Both sets of environments are based on environmental and orbital parameters provided by the ISS program; however, the SAGE III Mission Success environments are based on nominal orbital parameters that are expected during ISS operations whereas the ISS Extreme environments include the full envelope of possible ISS attitudes.

The ISS orbit has many parameters which can vary, including beta angle, yaw, pitch and roll. The design of the SAGE III payload must take into account the worst-case combinations of these parameters for the specific location of the payload on the ISS. The ranges for each of these parameters are shown in Table 1. These parameters were used as the bounds for selecting worst-case orbits for hot and cold cases on ELC-4 and on EOTP. By its nature as a transfer platform, the EOTP does not remain at the same location while SAGE III is attached. Therefore, it was necessary to determine the hottest and coldest EOTP locations for the SAGE III payload. A previously study considered four locations and determined the hottest location to be the second workstation aboard the MBS and the coldest location to be just outside the Dragon trunk.

Table 1: ISS Beta Angle and Attitude Ranges

	Beta		Yaw		Pitch		Roll	
	Min	Max	Min	Max	Min	Max	Min	Max
SAGE Mission Success	-75°	75°	-9°	-3°	-12°	-2°	0.5°	1°
ISS Extreme	-75°	75°	-15°	15°	-20°	15°	-15°	15°

3 Method

Thermal Desktop 5.5 Patch 13[3] and version 39a of the SAGE III System Thermal Model were used for this analysis. A user output file was created to output the temperatures at 14 nodes of interest. This facilitated the use of an Excel-based tool called FilePlottingTools, which was developed internally at LaRC by Salvatore Scola, to quickly process the results from each set of parametric runs.

A DoE table was first generated with all variables (beta, yaw, pitch & roll) normalized between -1 and 1. Because repeated points are not necessary for deterministic models, space-filling designs are standard practice for setting up computer experiments unless characteristics of the response are known in advance. Based on experience, the worst-case hot and cold locations were more likely to occur at extreme angles for beta, yaw, pitch, and roll. Therefore, a 2-level full factorial DoE with the four variables (16 runs) was created to capture all vertices of the 4-dimensional Euclidean design space. A space-filling sphere packing (also known as maximin) DoE, generated using JMP 10[4], was added to fill the interior of the design space. All points within a small Euclidean distance of the points at the vertices were removed to prevent wasted computational time from running duplicate or near-duplicate points. This DoE had the desired property of including all of the vertices of the design space while filling the interior evenly.

This normalized DoE was then scaled to generate DoEs for each set of cases (SAGE Mission Success and ISS Extreme) based on the actual limits for that set of cases. The two sets of cases were run at three locations—ELC-4 and the hottest and coldest EOTP locations—for a total of six sets of runs. The SAGE Mission Success cases at ELC-4 involved the additional complexity that SAGE III science (solar and lunar occultation) data is only taken between beta angles of -60° to +60°. To account for this, 16 additional runs were added to that DoE table to bound the narrower beta angle range for the science cases. Points with beta angles outside this range were ignored when determining hot and cold locations for science cases. The final SAGE Mission Success DoE table at ELC-4 had 79 runs, while all others had 64 runs each.

For all six sets of runs, all power and heaters were switched off so as not to mask temperature changes due to the external radiative environment. Therefore, all temperature differences between cases were solely due to differences in the orbital thermal environments (rather than, i.e., to differences in heater duty cycles).

The problem of finding the worst-case hot or worst-case cold combinations of beta, yaw, pitch and roll is inherently a multi-objective optimization problem, with the temperatures of the individual subsystems as objectives. Fortunately, the temperatures of the subsystems are highly correlated, which facilitated treating the problem as single-objective with an aggregate objective function to allow use of the EGO algorithm. The aggregate objective function used was the average of the steady-state temperatures of the 14 nodes listed in Table 2. These nodes were selected to include each electronics box as well as the flight thermal sensors on the Sensor Assembly (SA) that are mounted on critical components. Note that this aggregate objective function was used only to determine new points to run, not to decide which orbit out of all those run would serve as the hot or cold case for each particular component.

Table 2: Nodes Considered

Component	Node
CMP1	SAGE_CMP1.117
CMP2	SAGE_CMP2.117
DMP	SAGE_DMP.15
HEU	SAGE_HEXA.41405
HMA	SAGE_HEXA.44200
IAM	SAGE_IAM.2014
ICE	SAGE_ICE_BOX.692
SA: CCD Controller	SAGE_INSTRUMENT.1193
SA: Azimuth Motor	SAGE_INSTRUMENT.1701
SA: CCD	SAGE_INSTRUMENT.1773
SA: Scan Mirror	SAGE_INSTRUMENT.1988
SA: Attenuator	SAGE_INSTRUMENT.2033
SA: Elevation Motor	SAGE_INSTRUMENT.2036
SA: RVDT	SAGE_INSTRUMENT.2041

The EGO algorithm is summarized here along with adaptations for this problem. The EGO method is described in more detail by Jones, Schonlau, and Welch[2]. A stochastic process model was fit to the average temperature data. This type of surrogate model assumes that the errors (or deviations from the function mean value) at two points ($x^{(i)}$ and $x^{(j)}$) are correlated as

$$Corr[\epsilon(\mathbf{x}^{(i)}), \epsilon(\mathbf{x}^{(j)})] = \exp[-d(\mathbf{x}^{(i)}, \mathbf{x}^{(j)})]$$

where $d(\mathbf{x}^{(i)}, \mathbf{x}^{(j)})$ is the weighted distance given by

$$d(\mathbf{x}^{(i)}, \mathbf{x}^{(j)}) = \sum_{h=1}^{k} \theta_h \left| x_h^{(i)} - x_h^{(j)} \right|^{p_h}$$

Here k is the number of dimensions in the design space and θ_h and p_h are model parameters (thus there are twice as many model parameters as there dimensions in the design space). The surrogate model is fit to the data by varying these model parameters using a global optimizer to find the maximum likelihood[2]. The EGO code written for this work contains three choices for global optimization of the likelihood function: Simulated Annealing, Particle Swarm Optimization (PSO), and a multi-start approach using multiple runs of the Matlab built-in local optimizer called fmincon[5]. The local optimizer fmincon has several available algorithms. For this problem, the Sequential Quadratic Programming (SQP) algorithm was found to be effective. Initially, two of the three optimizers were chosen and the model parameters with the better likelihood value were used to fit the model. However, even with as few as 10 runs, the multi-start approach for finding the maximum likelihood was consistently able to find model parameters that were as good as or better than those found with the two global optimization methods. Therefore, for later iterations the much faster multi-start approach was typically the only optimizer used for this step.

Rather than find the maximum of the likelihood function, all optimizers were actually used to find the minimum of the negative natural logarithm of the likelihood function. Taking the natural logarithm of the likelihood function was found to cause faster convergence of the optimizer. Using the negative of this value was necessary for the fmincon function, which can only find local minima (the other two functions were user-programmed and have the capability to maximize or minimize the objective function).

After fitting model parameters, cross-validation checks were performed[2]. These checks involved leaving one point out of the dataset and then using the surrogate model with the other points to predict the value at the excluded point. The better the model fits the data, the closer the predicted value will be to the actual value at that point.

After the stochastic process model was fit and validated, the next step was to use the model to find the maximum of the expected improvement (EI), given by

$$E[I(\mathbf{x})] = (f_{min} - \hat{y})\Phi\left(\frac{f_{min} - \hat{y}}{s}\right) + s\varphi\left(\frac{f_{min} - \hat{y}}{s}\right)$$

where f_{min} is the current best value, $\hat{y}$ and s are the predicted value and standard error at $\mathbf{x}$, and $\Phi(\cdot)$ and $\varphi(\cdot)$ are the standard normal cumulative distribution and density functions[2]. This formula is for minimizing a function (cold case), but the EI formula for maximizing a function (hot case) is very similar. The derivation for the EI formula is discussed by Jones, Schonlau, and Welch[2]. The same three global optimizers as for fitting the surrogate model were used here (in various combinations) to maximize the expected improvement by varying the design variables (beta, yaw, pitch, and roll).

The term "improvement" as used here and in the remainder of this document refers to progress towards the optimization goals of finding orbits that result in the maximum and minimum temperatures (it does not imply that conditions are more favorable for SAGE III). For example, identifying a hot-case orbit with higher temperatures than the current hottest orbit would be considered improvement. The expected improvement can be conceptualized just the way it sounds—the amount of improvement in the current minimum or maximum value that can be expected (on average) by sampling the objective function at a given point. The use of EI as a metric balances exploration of the design space with exploitation of the available data. That is, the dependence on the standard error tends to increase the EI in regions away from sampled points (exploration), while the dependence on predicted value tends to increase the EI close

to the best current values (exploitation). The behavior of the Expected Improvement function is illustrated in Figure 4. Here an arbitrary 1D test function was sampled at the circled points and a surrogate model was fit to the data through these points. The expected improvement for finding the global minimum of this function, plotted in the same figure, has three significant maxima. The locations of these maxima show a balance between sampling near points with low values and sampling in regions of high uncertainty.
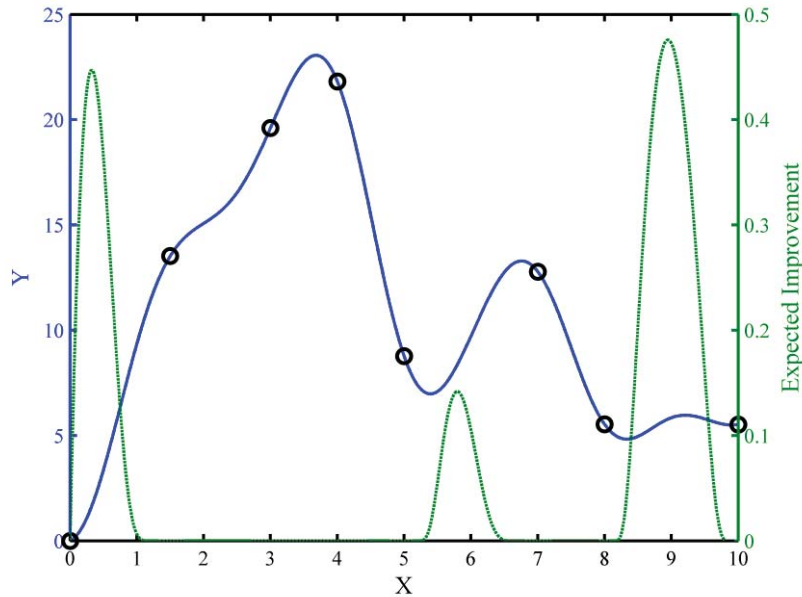
Figure 4: Example of Expected Improvement for unknown test function.

One of the disadvantages of the general Efficient Global Optimization approach is that, after the initial points in the space-filling DoE are completed, it is not amenable to parallel computing (or to conducting several runs overnight without intervention). Instead, after each new point, the surrogate model is fitted again with the new data, and the next point of maximum EI is chosen. This process is especially tedious in cases where the model is not integrated with the EGO code.

The Expected Improvement function is highly multimodal, often with numerous local maxima with values on the same order of magnitude but distant from each other in the design space (as shown in Figure 4). The addition of one more sampled point at the global maximum may cause only small shifts in the locations and expected improvement values of these other local maxima. In many cases, the next global maximum of expected improvement will be very close to one of the other local maxima from the previous iteration. Therefore, in cases where wall-clock time is critical, points should be tested at several of the largest local maxima of EI in parallel with the global maximum. Since the EGO implementation for this work already included a multi-start optimizer, it was easy to save the locations of several of the largest local EI maxima. This adaptation is highly recommended because it 1) facilitates parallel computing and 2) minimizes user interaction in cases where the model is not easy to integrate with the EGO code. For this work, the first benefit was not used, but the second was extremely helpful, particularly for setting points to run overnight.

A global expected improvement below 0.3°C for the average temperature was considered to signify convergence for this application. Note that this is the expected improvement from one more function evaluation, not the total remaining expected improvement for infinitely many function evaluations (finding the "true" optimum). This convergence threshold was selected to be small enough to provide the desired level of accuracy, but not so small as to require an excessive number of iterations. At least two iterations were conducted for each case because the EI can sometimes jump after the first iteration.

Although only the average temperature was used by the EGO algorithm, the hottest or coldest temperatures for the components do not always occur in the same run. Therefore, when selecting hot and cold cases, the temperatures of individual components were considered, not the average temperature. In order for an orbit to be considered hot or cold case orbit for a particular component, it must be within 2°C of the maximum or minimum temperature for that component. This 2°C requirement was selected as a compromise between accurately capturing the most severe temperatures and reducing the number of special cases required for individual subsystems. Fortunately, in most sets, the orbit with the most extreme average temperature was able to be used as the hot or cold case for all subsystems.

4   Results

4.1   SAGE Mission Success Cases

4.1.1   ELC-4

On ELC-4, the same set of runs was used for finding both the hot and cold cases. This allowed a single surrogate model to be fitted to the data. Then the maximization of expected improvement was run twice (flipping the sign of the average temperatures) to predict the new points for minimization and maximization of the average temperature. The EGO algorithm converged to both the hot and cold cases after 4 iterations and a total of 13 new runs (6 for cold and 7 for hot). This brought the total number of runs for ELC-4 SAGE Mission Success cases to 92.

Cross-validation of the surrogate model showed some undesirable behavior, such as an outlier. Despite this, the method successfully identified new hot and cold cases (that were more extreme than those in the initial DoE runs), and the expected improvement steadily decreased until convergence criteria were satisfied. Additionally, the temperatures of the 14 components considered were strongly correlated, which validates the choice of a single aggregate objective function. This lends confidence that the most extreme hot and cold orbits were successfully identified (to within the convergence tolerance).

The minimum temperatures for each component and the runs during which they occurred are shown in Table 3 (the specific nodes considered for each component are those shown in Table 2).

Table 4 shows the temperatures, and the differences from the overall minimum component temperatures, for the cold case from the DOE runs (run 19) and the final cold case after EGO convergence (run 90). The final cold case (run 90) is within 0.3°C of the minimum for each component, so no special cases are needed. Run 90 has only a slight average temperature improvement (in the optimization sense of minimizing the objective function) of 0.2°C compared to the cold case from the original DoE runs (run 19).

Table 3: Minimum Temperatures during ELC-4 SAGE Mission Success Cases

Component	Min Temp (°C)	Run #	Beta (°)	Yaw (°)	Pitch (°)	Roll (°)
CMP1	-27.8	90	-58.9	-8.4	-2.0	0.6
CMP2	-27.1	19	-60.0	-9.0	-2.0	1.0
DMP	-27.4	19	-60.0	-9.0	-2.0	1.0
HEU	-20.8	81	-56.3	-8.5	-2.0	0.9
HMA	-27.5	19	-60.0	-9.0	-2.0	1.0
IAM	-28.7	19	-60.0	-9.0	-2.0	1.0
ICE	-24.3	87	-58.7	-8.4	-2.0	0.8
CCD Controller	-28.3	90	-58.9	-8.4	-2.0	0.6
Azimuth Motor	-28.8	90	-58.9	-8.4	-2.0	0.6
CCD	-28.5	90	-58.9	-8.4	-2.0	0.6
Scan Mirror	-32.1	90	-58.9	-8.4	-2.0	0.6
Attenuator	-30.5	90	-58.9	-8.4	-2.0	0.6
Elevation Motor	-31.0	90	-58.9	-8.4	-2.0	0.6
RVDT	-31.0	90	-58.9	-8.4	-2.0	0.6

Table 4: SAGE Mission Success ELC-4 Cold Case Temperatures

	Temps in each min case (°C)		Difference from min (°C)	
Cold Case	DoE Runs	Final Cold Case	DoE Runs	Final Cold Case
Run #	19	90	19	90
CMP1	-27.8	-27.8	0.0	0.0
CMP2	-27.1	-27.0	0.0	0.1
DMP	-27.4	-27.4	0.0	0.1
HEU	-20.2	-20.5	0.6	0.3
HMA	-27.5	-27.5	0.0	0.0
IAM	-28.7	-28.7	0.0	0.0
ICE	-23.9	-24.2	0.4	0.1
CCD Controller	-28.2	-28.3	0.1	0.0
Azimuth Motor	-28.6	-28.8	0.2	0.0
CCD	-28.3	-28.5	0.2	0.0
Scan Mirror	-31.9	-32.1	0.2	0.0
Attenuator	-30.2	-30.5	0.2	0.0
Elevation Motor	-30.7	-31.0	0.3	0.0
RVDT	-30.7	-31.0	0.3	0.0

Temps within 0.4°C of min are highlighted

Differences of >2°C are highlighted

The maximum temperatures for each component and the runs during which they occurred are shown in Table 5. Table 6 shows the temperatures, and the differences from the overall maximum component temperatures, for the hot case from the DOE runs (run 33) and the final hot case after EGO convergence (run 91). The final hot case (run 91) is within 0.4°C of the maximum for each component, so no special cases are needed. Run 91 has a fairly significant average temperature improvement of 1.9°C compared to the hot case from just the original DoE runs (run 33).

Table 5: Maximum Temperatures during ELC-4 SAGE Mission Success Cases

Component	Max Temp (°C)	Run #	Beta (°)	Yaw (°)	Pitch (°)	Roll (°)
CMP1	3.8	89	43.6	-7.6	-6.1	0.5
CMP2	15.6	89	43.6	-7.6	-6.1	0.5
DMP	15.9	89	43.6	-7.6	-6.1	0.5
HEU	-0.1	91	43.6	-8.4	-3.7	0.5
HMA	9.0	91	43.6	-8.4	-3.7	0.5
IAM	7.7	89	43.6	-7.6	-6.1	0.5
ICE	2.4	91	43.6	-8.4	-3.7	0.5
CCD Controller	-3.4	91	43.6	-8.4	-3.7	0.5
Azimuth Motor	-6.8	91	43.6	-8.4	-3.7	0.5
CCD	-6.4	91	43.6	-8.4	-3.7	0.5
Scan Mirror	-1.1	91	43.6	-8.4	-3.7	0.5
Attenuator	-2.3	91	43.6	-8.4	-3.7	0.5
Elevation Motor	-0.5	91	43.6	-8.4	-3.7	0.5
RVDT	-0.8	91	43.6	-8.4	-3.7	0.5

Table 6: SAGE Mission Success ELC-4 Hot Case Temperatures

Hot Case	Temps in each max case (°C)		Difference from max (°C)	
	DoE Runs	Final Hot Case	DoE Runs	Final Hot Case
Run #	33	91	33	91
CMP1	2.1	3.4	-1.6	-0.3
CMP2	13.0	15.4	-2.6	-0.3
DMP	13.4	15.6	-2.5	-0.3
HEU	-1.7	-0.1	-1.6	0.0
HMA	6.7	9.0	-2.3	0.0
IAM	5.9	7.3	-1.9	-0.4
ICE	-0.1	2.4	-2.5	0.0
CCD Controller	-5.8	-3.4	-2.4	0.0
Azimuth Motor	-9.0	-6.8	-2.2	0.0
CCD	-8.8	-6.4	-2.3	0.0
Scan Mirror	-2.9	-1.1	-1.8	0.0
Attenuator	-4.0	-2.3	-1.7	0.0
Elevation Motor	-2.1	-0.5	-1.5	0.0
RVDT	-1.8	-0.8	-1.0	0.0

Temps within 0.4°C of max are highlighted	Differences of >2°C are highlighted

4.1.2   EOTP

The EOTP cold case was comparatively slow to converge, requiring 5 iterations and 13 new cases. This brought the total number of runs for EOTP cold cases to 77. Cross-validation of the surrogate model showed no major problems. Additionally, the temperatures of the 14 components considered were strongly correlated, which validates the use of a single aggregate objective function. This gives confidence that the most extreme cold orbit was successfully identified (to within the convergence tolerance).

The minimum temperatures for each component and the runs during which they occurred are shown in Table 7. Table 8 shows the temperatures, and the differences from the overall minimum component temperatures, for the cold case from the DoE runs (run 26) and the final cold case after EGO convergence (run 71). The final cold case (run 71) is within 0.3°C of the minimum for each component, so no special cases are needed. Run 71 has an average temperature improvement of 1.2°C compared to the cold case from just the original DOE runs (run 26).

Table 7: Minimum Temperatures during EOTP Cold SAGE Mission Success Cases

Component	Min Temp (°C)	Run #	Beta (°)	Yaw (°)	Pitch (°)	Roll (°)
CMP1	-39.1	71	-3.3	-5.8	-12.0	0.5
CMP2	-39.1	71	-3.3	-5.8	-12.0	0.5
DMP	-38.5	71	-3.3	-5.8	-12.0	0.5
HEU	-37.5	71	-3.3	-5.8	-12.0	0.5
HMA	-39.6	71	-3.3	-5.8	-12.0	0.5
IAM	-39.0	71	-3.3	-5.8	-12.0	0.5
ICE	-39.6	71	-3.3	-5.8	-12.0	0.5
CCD Controller	-42.4	74	-0.9	-5.4	-12.0	0.5
Azimuth Motor	-42.8	74	-0.9	-5.4	-12.0	0.5
CCD	-42.7	74	-0.9	-5.4	-12.0	0.5
Scan Mirror	-42.5	74	-0.9	-5.4	-12.0	0.5
Attenuator	-42.3	74	-0.9	-5.4	-12.0	0.5
Elevation Motor	-42.0	74	-0.9	-5.4	-12.0	0.5
RVDT	-42.1	74	-0.9	-5.4	-12.0	0.5

Table 8: SAGE Mission Success EOTP Cold Case Temperatures

	Temps in each min case (°C)		Difference from min (°C)	
Cold Case	DoE Runs	Final Cold Case	DoE Runs	Final Cold Case
Run #	26	71	26	71
CMP1	-37.5	-39.1	1.6	0.0
CMP2	-37.6	-39.1	1.6	0.0
DMP	-36.9	-38.5	1.5	0.0
HEU	-36.1	-37.5	1.3	0.0
HMA	-38.4	-39.6	1.3	0.0
IAM	-37.4	-39.0	1.5	0.0
ICE	-38.8	-39.6	0.8	0.0
CCD Controller	-41.5	-42.3	0.8	0.1
Azimuth Motor	-41.9	-42.7	0.9	0.1
CCD	-41.9	-42.6	0.8	0.1
Scan Mirror	-40.6	-42.2	1.9	0.3
Attenuator	-40.7	-42.1	1.6	0.2
Elevation Motor	-40.2	-41.8	1.8	0.2
RVDT	-40.2	-41.8	1.9	0.3

Temps within 0.4°C of min are highlighted

Differences of >2°C are highlighted

The EOTP hot case converged after only two iterations of one run each, bringing the total number of runs for SAGE Mission Success EOTP hot cases to 66. Cross-validation of the surrogate model showed no major problems. The temperatures of the 14 components considered were correlated, though not as strongly as in the previous cases. The EGO algorithm successfully identified new hot cases, and the maximum expected improvement decreased rapidly after each new run. This gives confidence that the most extreme hot orbit was successfully identified (to within the convergence tolerance).

The maximum temperatures for each component and the runs during which they occurred are shown in Table 9. Table 10 shows the temperatures, and the differences from the overall maximum component temperatures, for final hot case after EGO convergence (run 65) and the two hot cases from the DOE runs (run 53 for Sensor Assembly (SA) and run 9 for everything else). With only two iterations of one additional run each, the EGO algorithm was able to locate a new hot case that increased the average temperature by 1°C and eliminated the need for a separate hot case for the SA. This represents a significant improvement with very little extra investment.

Table 9: Maximum Temperatures during EOTP Hot SAGE Mission Success Cases

Component	Max Temp (°C)	Run #	Beta (°)	Yaw (°)	Pitch (°)	Roll (°)
CMP1	7.9	65	75.0	-8.3	-12.0	0.7
CMP2	3.1	65	75.0	-8.3	-12.0	0.7
DMP	7.2	65	75.0	-8.3	-12.0	0.7
HEU	7.3	65	75.0	-8.3	-12.0	0.7
HMA	4.6	65	75.0	-8.3	-12.0	0.7
IAM	10.5	65	75.0	-8.3	-12.0	0.7
ICE	-3.1	65	75.0	-8.3	-12.0	0.7
CCD Controller	-1.6	65	75.0	-8.3	-12.0	0.7
Azimuth Motor	3.8	65	75.0	-8.3	-12.0	0.7
CCD	-1.6	65	75.0	-8.3	-12.0	0.7
Scan Mirror	52.5	64	75.0	-9.0	-12.0	0.6
Attenuator	41.0	64	75.0	-9.0	-12.0	0.6
Elevation Motor	53.3	64	75.0	-9.0	-12.0	0.6
RVDT	52.8	64	75.0	-9.0	-12.0	0.6

Table 10: SAGE Mission Success EOTP Hot Case Temperatures

	Temps in each max case (°C)			Difference from max (°C)		
Hot Case	**Overall Hot Case (DoE)**	**SA Hot Case (DoE)**	**Final Overall Hot Case**	**Overall Hot Case (DoE)**	**SA Hot Case (DoE)**	**Final Overall Hot Case**
Run #	**9**	**53**	**65**	**9**	**53**	**65**
CMP1	7.4	6.3	7.9	-0.6	-1.7	0.0
CMP2	2.5	1.5	3.1	-0.6	-1.6	0.0
DMP	6.5	5.3	7.2	-0.6	-1.9	0.0
HEU	7.2	6.8	7.3	0.0	-0.5	0.0
HMA	4.1	2.7	4.6	-0.5	-1.9	0.0
IAM	9.7	8.3	10.5	-0.9	-2.2	0.0
ICE	-3.4	-4.1	-3.1	-0.4	-1.0	0.0
CCD Controller	-1.7	-3.4	-1.6	-0.1	-1.8	0.0
Azimuth Motor	3.3	2.3	3.8	-0.5	-1.5	0.0
CCD	-1.7	-3.3	-1.6	-0.1	-1.7	0.0
Scan Mirror	48.3	51.7	51.9	-4.1	-0.8	-0.6
Attenuator	37.8	40.2	40.6	-3.2	-0.8	-0.4
Elevation Motor	49.1	52.6	52.7	-4.2	-0.7	-0.6
RVDT	48.6	52.2	52.2	-4.2	-0.6	-0.7

Temps within 0.4°C of max are highlighted   Differences of >2°C are highlighted

4.1.3 Summary

The overall hot and cold case orbits for SAGE Mission Success cases are shown in Table 11. The beta angle for solar and lunar science event measurements is limited to +/-60° (since the ISS only passes through orbit shadow in this beta angle range), while all other orbits such as standby and those with only limb events can occur over the entire beta angle range of +/-75°. The beta angles for both the hot and cold cases on ELC-4 fell within the -60° to 60° range for both science and standby cases, so separate orbits were not required for science and standby cases.

Table 11: SAGE Mission Success Worst-Case Orbits

	ELC-4 (Science & Standby)		EOTP	
	Hot	**Cold**	**Hot**	**Cold**
Beta	43.6°	-58.9°	75.0°	-3.3°
Yaw	-8.4°	-8.4°	-8.3°	-5.8°
Pitch	-3.7°	-2.0°	-12.0°	-12.0°
Roll	0.5°	0.6°	0.7°	0.5°

4.2 ISS Extreme Cases

4.2.1 ELC-4

As for SAGE Mission Success ELC-4 cases, the same set of runs was used for finding both the ISS Extreme ELC-4 hot and cold cases. The EGO algorithm converged to both the hot and cold cases after 3 iterations and a total of 12 new runs (7 for cold and 5 for hot). This brought the total number of runs for ELC-4 ISS Extreme cases to 76.

The temperatures of the 14 nodes considered were not always strongly correlated, resulting in the need for special cases for certain components. This means that the use of the aggregate objective function is not perfect, but still serves as a useful tool for the EGO algorithm. Despite this, cross-validation of the surrogate model showed an excellent fit for the average temperatures, and the expected improvement steadily decreased. This lends confidence that the most extreme overall hot and cold orbits were successfully identified (to within the convergence tolerance).

The minimum temperatures for each component, and the runs during which they occurred, are shown in Table 12. Table 13 shows the temperatures, and the differences from the overall minimum component temperatures, for the final cold case after EGO convergence (run 74), the overall cold case from only the DOE runs (run 3), and the ICE cold case (run 5). The final cold case (run 74) has an average temperature improvement of 0.3°C compared to the cold case for the original DOE runs (run 3), and does not eliminate the need for a separate ICE cold case (run 5).

Table 12: Minimum Temperatures during ELC-4 ISS Extreme Cases

Component	Min Temp (°C)	Run #	Beta (°)	Yaw (°)	Pitch (°)	Roll (°)
CMP1	-37.2	74	-75.0	-15.0	15.0	13.9
CMP2	-34.4	74	-75.0	-15.0	15.0	13.9
DMP	-35.5	74	-75.0	-15.0	15.0	13.9
HEU	-31.7	74	-75.0	-15.0	15.0	13.9
HMA	-35.4	74	-75.0	-15.0	15.0	13.9
IAM	-38.3	74	-75.0	-15.0	15.0	13.9
ICE	-33.6	5	-75.0	15.0	-20.0	15.0
CCD Controller	-35.5	74	-75.0	-15.0	15.0	13.9
Azimuth Motor	-36.1	74	-75.0	-15.0	15.0	13.9
CCD	-35.6	74	-75.0	-15.0	15.0	13.9
Scan Mirror	-42.1	72	-75.0	-14.8	15.0	13.2
Attenuator	-39.4	72	-75.0	-14.8	15.0	13.2
Elevation Motor	-40.5	72	-75.0	-14.8	15.0	13.2
RVDT	-40.5	72	-75.0	-14.8	15.0	13.2

Table 13: ISS Extreme ELC-4 Cold Case Temperatures

Cold Case	Temps in each min case (°C)			Difference from min (°C)		
	DoE Runs Only	ICE Cold Case	Final Cold Case	DoE Runs Only	ICE Cold Case	Final Cold Case
Run #	3	5	74	3	5	74
CMP1	-36.9	-30.0	-37.2	0.3	7.2	0.0
CMP2	-34.3	-31.0	-34.4	0.1	3.4	0.0
DMP	-35.3	-30.2	-35.5	0.2	5.3	0.0
HEU	-30.8	-28.3	-31.7	0.9	3.3	0.0
HMA	-35.2	-30.8	-35.4	0.2	4.6	0.0
IAM	-38.1	-30.3	-38.3	0.3	8.1	0.0
ICE	-29.2	-33.6	-29.5	4.3	0.0	4.1
CCD Controller	-35.3	-32.2	-35.5	0.2	3.3	0.0
Azimuth Motor	-35.9	-32.5	-36.1	0.2	3.6	0.0
CCD	-35.4	-32.4	-35.6	0.2	3.2	0.0
Scan Mirror	-41.7	-32.9	-41.9	0.4	9.2	0.1
Attenuator	-39.1	-32.5	-39.4	0.3	6.9	0.0
Elevation Motor	-40.1	-32.5	-40.4	0.3	7.9	0.1
RVDT	-40.1	-32.6	-40.4	0.4	7.9	0.1
	Temps within 0.4°C of min are highlighted			Differences of >2°C are highlighted		

The maximum temperatures for each component, and the runs during which they occurred, are shown in Table 14. Table 15 shows the temperatures, and the differences from the overall maximum component temperatures, for overall hot case (run 9), the HEU hot case (run 4), and the ICE hot case (run 11). No new hot cases were found with the EGO algorithm. This is unsurprising, since the overall hot case occurs on a vertex of its design space. Therefore, it was already included in the initial DoE runs (whereas the DoE runs would likely not hit a maximum inside the design space precisely). However, the convergence of the EGO algorithm still serves to increase confidence that the true overall hot case was identified.

Table 14: Maximum Temperatures during ELC-4 ISS Extreme Cases

Component	Max Temp (°C)	Run #	Beta (°)	Yaw (°)	Pitch (°)	Roll (°)
CMP1	7.8	9	75.0	-15.0	-20.0	15.0
CMP2	12.9	11	75.0	-15.0	15.0	15.0
DMP	12.8	9	75.0	-15.0	-20.0	15.0
HEU	10.1	4	-75.0	15.0	-20.0	-15.0
HMA	9.7	9	75.0	-15.0	-20.0	15.0
IAM	10.2	9	75.0	-15.0	-20.0	15.0
ICE	3.2	11	75.0	-15.0	15.0	15.0
CCD Controller	3.3	9	75.0	-15.0	-20.0	15.0
Azimuth Motor	1.8	9	75.0	-15.0	-20.0	15.0
CCD	1.8	9	75.0	-15.0	-20.0	15.0
Scan Mirror	5.5	9	75.0	-15.0	-20.0	15.0
Attenuator	5.3	9	75.0	-15.0	-20.0	15.0
Elevation Motor	7.2	9	75.0	-15.0	-20.0	15.0
RVDT	6.4	9	75.0	-15.0	-20.0	15.0

Table 15: ISS Extreme ELC-4 Hot Case Temperatures

	Temps in each max case (°C)			Difference from max (°C)		
Hot Case	**HEU Hot Case**	**Overall Hot Case**	**ICE Hot Case**	**HEU Hot Case**	**Overall Hot Case**	**ICE Hot Case**
Run #	**4**	**9**	**11**	**4**	**9**	**11**
CMP1	-0.5	7.8	2.1	-8.4	0.0	-5.8
CMP2	-5.0	12.5	12.9	-17.8	-0.3	0.0
DMP	-2.4	12.8	10.9	-15.1	0.0	-1.8
HEU	10.1	5.4	1.4	0.0	-4.7	-8.7
HMA	-2.9	9.7	7.7	-12.6	0.0	-2.0
IAM	-0.5	10.2	4.2	-10.7	0.0	-6.0
ICE	-5.3	0.4	3.2	-8.5	-2.8	0.0
CCD Controller	-5.6	3.3	0.8	-8.9	0.0	-2.5
Azimuth Motor	-5.2	1.8	-2.2	-6.9	0.0	-4.0
CCD	-5.9	1.8	-1.1	-7.7	0.0	-2.8
Scan Mirror	2.4	5.5	-9.5	-3.1	0.0	-15.0
Attenuator	1.2	5.3	-6.3	-4.2	0.0	-11.6
Elevation Motor	3.4	7.2	-7.2	-3.8	0.0	-14.3
RVDT	4.1	6.4	-7.5	-2.3	0.0	-13.9

Temps within 0.4°C of max are highlighted

Differences of >2°C are highlighted

4.2.2   EOTP

The ISS Extreme EOTP Cold case did not converge to the convergence criterion of EI less than 0.3°C. The EI decreased from as high as 8.6°C to below 1°C after the first few iterations. After this, the EI did not converge further. Cross-validation of the model showed several outliers, as well as an apparent correlation between the residuals and the objective function values, indicating non-ideal model fit. This may be due to the location of the payload outside of the Dragon trunk. In this location, at certain angles ISS solar panels can rotate to block (or partially block) the payload's view of the sun, as shown in Figure 5 and Figure 6. This leads to a highly multi-modal response, sharp temperature variations, and lack of correlation between the 14 component temperatures. All of these factors cause difficulty when fitting the surrogate model.

Six iterations were conducted for a total of 59 additional runs. This brought the total number of runs for EOTP Cold ISS Extreme cases to 124. This large number of runs was not strictly necessary, since the convergence threshold of 0.3°C could likely have been increased to require fewer runs while still retaining an acceptable level of accuracy. Furthermore, examination of the results showed a consistent overestimation of the expected improvement; and no new cold cases were identified in the last 34 runs. Runs were continued to examine the convergence behavior of the EGO algorithm in a difficult case such as this.

The minimum temperatures for each component, and the runs during which they occurred, are shown in Table 16. Unlike in any other case, the minimum temperatures for the components considered occur at three very different beta angles and at different values spanning the ranges for yaw, pitch and roll. This indicates that, as mentioned, the temperature response is highly multimodal, likely due to the location of SAGE III in relation to the ISS solar panels. These solar panels rotate to track the sun and can therefore block direct sunlight at many different beta angles and ISS attitudes, making the temperature dependence on these angles much more complicated and multi-modal. Like any optimization approach, EGO has difficulties finding the global optimum when there are numerous local optima; especially if the objective function values at these local optima are very close to the global optimum.

The temperatures of the 14 components are also not very strongly correlated, as shown in Table 17. This made the use of an aggregate objective function much less effective and contributed to the difficulties of using the EGO approach. Run 89 is the overall cold case, while run 58 is the cold case for CMP2, DMP, HEU, and ICE. It would be more concise to refer to run 58 as the overall cold case and run 89 as the cold case for the SA; however, run 89 is a much better overall cold case since it is within 5°C of the minimum for every component (whereas run 58 is almost 40°C above the minimum for some SA components). Run 23 was the overall cold case from only the DoE runs and still has the minimum temperature for some SA components (but run 89 is within the 2°C tolerance for accepting it as the cold case for those components).

Table 16: Minimum Temperatures during EOTP Cold ISS Extreme Cases

Component	Min Temp (°C)	Run #	Beta (°)	Yaw (°)	Pitch (°)	Roll (°)
CMP1	-42.3	89	-4.3	-7.0	-3.3	15.0
CMP2	-43.8	58	75.0	15.0	15.0	-8.7
DMP	-43.0	58	75.0	15.0	15.0	-8.7
HEU	-44.7	58	75.0	15.0	15.0	-8.7
HMA	-42.7	58	75.0	15.0	15.0	-8.7
IAM	-42.3	89	-4.3	-7.0	-3.3	15.0
ICE	-45.8	58	75.0	15.0	15.0	-8.7
CCD Controller	-44.3	89	-4.3	-7.0	-3.3	15.0
Azimuth Motor	-44.8	89	-4.3	-7.0	-3.3	15.0
CCD	-44.6	89	-4.3	-7.0	-3.3	15.0
Scan Mirror	-47.5	23	-74.2	-1.0	-20.0	15.0
Attenuator	-45.9	23	-74.2	-1.0	-20.0	15.0
Elevation Motor	-46.4	23	-74.2	-1.0	-20.0	15.0
RVDT	-46.6	23	-74.2	-1.0	-20.0	15.0

Table 17: ISS Extreme EOTP Cold Case Temperatures

Cold Case	Temps in each min case (°C)			Difference from min (°C)		
	Cold Case from DoE Runs Only	CMP2, DMP, HEU & ICE Cold Case	Final Overall Cold Case	Cold Case from DoE Runs Only	CMP2, DMP, HEU & ICE Cold Case	Final Overall Cold Case
Run #	23	58	89	23	58	89
CMP1	-41.8	-42.2	-42.3	0.5	0.1	0.0
CMP2	-37.6	-43.8	-41.5	6.1	0.0	2.3
DMP	-38.5	-43.0	-41.3	4.5	0.0	1.7
HEU	-39.8	-44.7	-40.3	5.0	0.0	4.4
HMA	-39.6	-42.7	-42.2	3.1	0.0	0.5
IAM	-41.5	-41.7	-42.3	0.8	0.6	0.0
ICE	-34.9	-45.8	-41.2	10.9	0.0	4.6
CCD Controller	-42.5	-42.8	-44.3	1.9	1.5	0.0
Azimuth Motor	-43.5	-38.5	-44.8	1.4	6.4	0.0
CCD	-43.0	-41.7	-44.6	1.7	3.0	0.0
Scan Mirror	-47.5	-9.2	-46.1	0.0	38.3	1.5
Attenuator	-45.9	-16.7	-45.4	0.0	29.2	0.5
Elevation Motor	-46.4	-9.5	-45.4	0.0	36.8	0.9
RVDT	-46.6	-9.7	-45.5	0.0	37.0	1.2

Temps within 0.4°C of min are highlighted   Differences of >2°C are highlighted

Run 58 appears to be unusual because it is the coldest case for most non-SA components but yet is nearly 40°C warmer than the coldest temperatures for some SA nodes. Further investigation of this case by viewing its orbit in Thermal Desktop revealed that for 5 of its 16 orbital positions, solar panels blocked direct sunlight from almost all of SAGE III except for the SA. The drastic difference between SA temperatures and the temperatures of the other nodes in this case is a result of this phenomenon. Screenshots of two of these orbital positions, viewed from the sun are shown in Figure 5 and Figure 6.
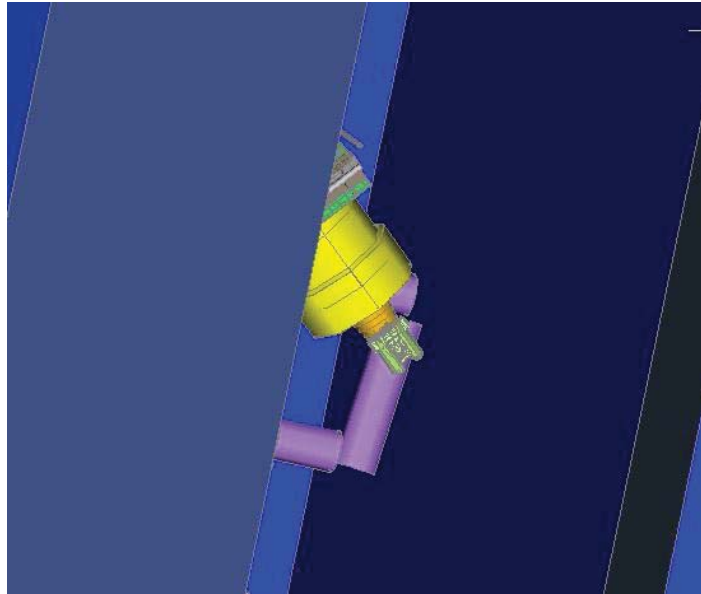

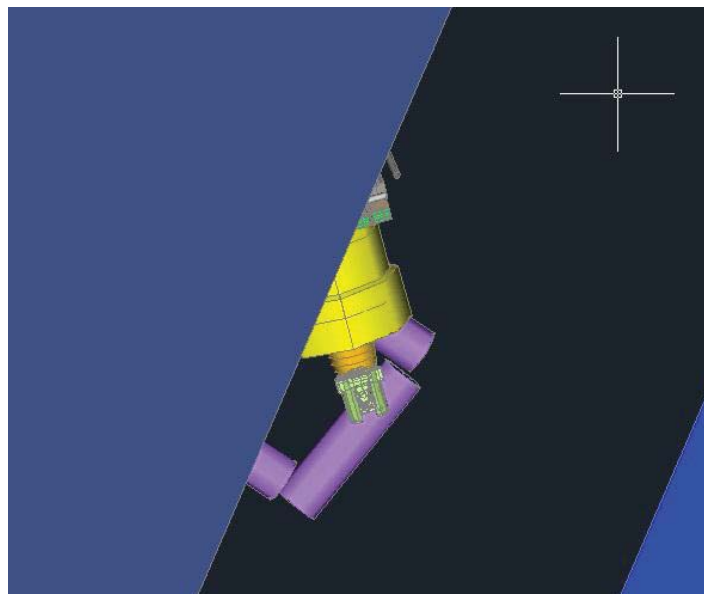**Figure 5: Run 58 orbital position (true anomaly = 225°) viewed from the sun.**

Figure 6: Run 58 orbital position (true anomaly = 202.5°) viewed from the sun.

The ISS Extreme EOTP hot case converged after 3 iterations for a total of 5 new runs. The total number of runs for SAGE Mission Success EOTP hot cases was 69. Cross-validation of the surrogate model

showed no major problems. The temperatures of the 14 nodes considered were strongly correlated, which validates the choice of a single aggregate objective function. The EGO algorithm successfully identified a hot case, and the maximum EI decreased after each new run. This gives confidence that the most extreme hot orbit was successfully identified (to within the convergence tolerance).

The maximum temperatures for each component and the runs during which they occurred are shown in Table 18. Table 19 shows the temperatures, and the differences from the overall maximum component temperatures, for final hot case after EGO convergence (run 65) and the hot cases from only the DoE runs (run 10). The final hot case (run 65) is within 0.5°C of the maximum for each component, so no special cases are needed. Run 65 has an average temperature improvement of 1.3°C compared to the hot case from just the original DoE runs (run 10).

Table 18: Maximum Temperatures during EOTP Hot ISS Extreme Cases

Component	Max Temp (°C)	Run #	Beta (°)	Yaw (°)	Pitch (°)	Roll (°)
CMP1	20.1	65	75.0	-15.0	-4.1	-15.0
CMP2	18.4	65	75.0	-15.0	-4.1	-15.0
DMP	21.7	65	75.0	-15.0	-4.1	-15.0
HEU	17.4	65	75.0	-15.0	-4.1	-15.0
HMA	18.6	65	75.0	-15.0	-4.1	-15.0
IAM	23.5	65	75.0	-15.0	-4.1	-15.0
ICE	8.8	65	75.0	-15.0	-4.1	-15.0
CCD Controller	11.4	65	75.0	-15.0	-4.1	-15.0
Azimuth Motor	15.8	65	75.0	-15.0	-4.1	-15.0
CCD	10.8	65	75.0	-15.0	-4.1	-15.0
Scan Mirror	62.9	10	75.0	-15.0	15.0	-15.0
Attenuator	51.6	65	75.0	-15.0	-4.1	-15.0
Elevation Motor	64.1	10	75.0	-15.0	15.0	-15.0
RVDT	63.3	10	75.0	-15.0	15.0	-15.0

Table 19: ISS Extreme EOTP Hot Case Temperatures

Hot Case	Temps in each max case		Difference from max	
	DoE Runs	Final Hot Case	DoE Runs	Final Hot Case
Run #	10	65	10	65
CMP1	17.9	20.1	-2.2	0.0
CMP2	16.6	18.4	-1.8	0.0
DMP	19.8	21.7	-1.9	0.0
HEU	15.5	17.4	-1.9	0.0
HMA	16.7	18.6	-1.9	0.0
IAM	21.2	23.5	-2.3	0.0
ICE	7.2	8.8	-1.6	0.0
CCD Controller	9.5	11.4	-1.9	0.0
Azimuth Motor	14.3	15.8	-1.5	0.0
CCD	8.9	10.8	-1.8	0.0
Scan Mirror	62.9	62.6	0.0	-0.3
Attenuator	51.6	51.6	0.0	0.0
Elevation Motor	64.1	63.5	0.0	-0.5
RVDT	63.3	62.9	0.0	-0.4

Temps within 0.4°C of max are highlighted — Differences of >2°C are highlighted

4.2.3 Summary

The overall hot and cold case orbits for ISS Extreme cases are shown in Table 20. All cases except for the EOTP hot case required separate cases for individual subsystems. These special cases are shown in Table 21.

Table 20: ISS Extreme Worst-Case Orbits

	ELC-4		EOTP	
	Hot*	Cold*	Hot	Cold*
Beta	75.0°	-75.0°	75.0°	-4.3°
Yaw	-15.0°	-15.0°	-15.0°	-7.0°
Pitch	-20.0°	15.0°	-4.1°	-3.3°
Roll	15.0°	13.9°	-15.0°	15.0°

* Require separate cases for specific subsystems.

Table 21: ISS Extreme Special Hot and Cold Cases

	ELC-4			EOTP
	ICE Hot	**HEU Hot**	**ICE Cold****	**CMP2, DMP, HEU & ICE Cold**
Beta	75.0°	-75.0°	-75.0°	75.0°
Yaw	-15.0°	15.0°	15.0°	15.0°
Pitch	15.0°	-20.0°	-20.0°	15.0°
Roll	15.0°	-15.0°	15.0°	-8.7°

**This case was later removed because after including heaters the differences from the overall cold case were no longer significant

5   Comparison with Previous Worst-Case Orbits

Table 22 shows a comparison of new orbit for the SAGE extreme hot op science case with the previous orbit. Similarly, Table 23 and Table 24 show comparisons for the SAGE hot op limb and SAGE hot survival EOTP cases, respectively. The SAGE hot survival ELC case is not shown because it has the same orbit as the SAGE hot op limb case. Highlighted cells mark instances in which predictions come within 15°C of the hardware limits. Changes of greater than 5°C between previous and new orbits are shown in bold.

The orbit-averaged ExPRESS Pallet Adapter (ExPA) temperature distributions for the previous and new SAGE hot survival EOTP cases are shown in Figure 7 and Figure 8, respectively. The large temperature differences shown in those figures explain why the largest temperature differences for the SAGE hot survival EOTP case occur for components (such as IAM, DMP, and CMP2) that have strong conductive ties to ExPA.

Table 22: Comparison of New and Previous SAGE Extreme Hot Op Sci Cases

	Limits (°C)	New Extreme Hot Op Sci	Previous Extreme Hot Op Sci	Change
Orbital Elements (°)				
Beta		43.6	60.0	
Yaw		-8.4	-3.0	
Pitch		-3.7	-2.0	
Roll		0.5	0.5	
Temperatures (°C)				
Elevation Motor	60	50.3	50.8	-0.5
Scan Mirror	60	45.3	44.8	0.5
Attenuator	60	45.1	43.1	2.0
RVDT	55	42.3	42.3	0.0
Azimuth Motor Stator	55	**32.3**	**25.1**	**7.2**
CCD	35	18.6	21.1	-2.5
CCD Controller PWA	55	**42.2**	**33.8**	**8.4**
HMA	60	**40.7**	**30.0**	**10.8**
HEU	60	**51.1**	**44.7**	**6.4**
ICE	60	**42.6**	**36.1**	**6.5**
IAM	65	**45.7**	**35.9**	**9.8**
CMP1	75	**42.3**	**34.4**	**7.9**
CMP2	75	**43.3**	**30.0**	**13.2**
DMP	65	**47.6**	**35.0**	**12.7**

Breaks 15°C margin

Table 23: Comparison of New and Previous SAGE Hot Op Limb Cases

	Limits (°C)	New	Previous		Change
		Hot Op Limb	Hot Op Limb	Hot Op Limb (HEU)	
Orbital Elements (°)					
Beta		43.6	60.0	-75.0	
Yaw		-8.4	-3.0	-9.0	
Pitch		-3.7	-2.0	-12.0	
Roll		0.5	0.5	0.5	
Temperatures (°C)					
Elevation Motor	60	41.6	39.1	40.3	1.3
Scan Mirror	60	37.3	34.6	35.9	1.4
Attenuator	60	31.5	28.5	28.9	2.6
RVDT	55	35.5	33.0	34.3	1.2
Azimuth Motor Stator	55	27.8	23.9	21.8	3.9
CCD	35	17.3	13.5	10.2	3.8
CCD Controller PWA	55	**40.4**	**35.3**	28.8	**5.1**
HMA	60	**40.4**	**32.6**	16.1	**7.8**
HEU	60	51.2	46.2	47.2	4.0
ICE	60	**45.8**	**40.4**	32.5	**5.4**
IAM	65	**45.9**	**38.4**	20.9	**7.5**
CMP1	75	**42.3**	**36.3**	25.1	**6.1**
CMP2	75	**43.4**	**32.8**	8.7	**10.6**
DMP	65	**47.8**	**38.0**	13.4	**9.8**

Breaks 15°C margin

27

Table 24: Comparison of New and Previous SAGE Hot Survival EOTP Cases

|	Limits (°C)	New Hot Survival EOTP	Previous Hot Survival EOTP	Change
Orbital Elements (°)				
Beta		75.0	-75.0	
Yaw		-8.3	-6.0	
Pitch		-12.0	-6.0	
Roll		0.7	0.9	
Temperatures (°C)				
Elevation Motor	85	**5.8**	**-2.2**	**8.0**
Scan Mirror	85	**6.0**	**-2.7**	**8.7**
Attenuator	60	**9.5**	**3.6**	**5.9**
RVDT	125	**5.5**	**-2.7**	**8.2**
Azimuth Motor Stator	65	20.0	19.6	0.4
CCD	65	18.9	18.5	0.4
CCD Controller PWA	65	19.5	18.5	1.0
HMA	80	18.2	15.0	3.2
HEU	80	**15.3**	**8.7**	**6.6**
ICE	65	0.9	-3.0	3.9
IAM	113	**21.5**	**-6.9**	**28.4**
CMP1	113	**18.0**	**-9.5**	**27.5**
CMP2	113	**11.9**	**-8.3**	**20.2**
DMP	75	**18.6**	**-2.7**	**21.3**
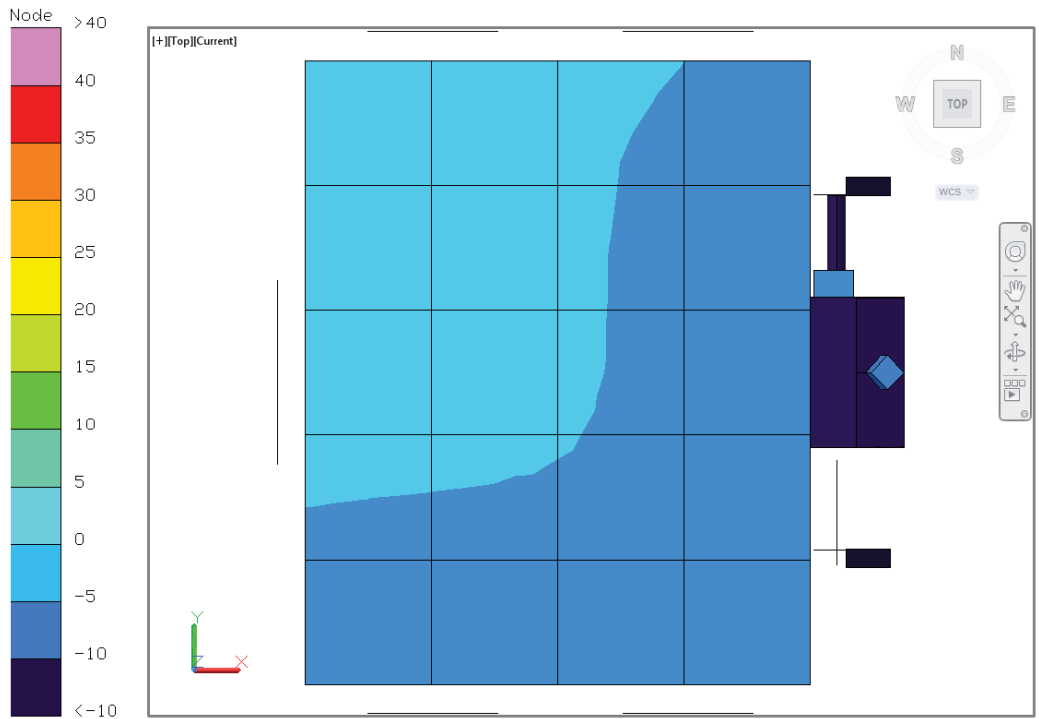
Figure 7: Orbit-averaged ExPA temperature distribution (°C) for previous SAGE hot survival EOTP case.

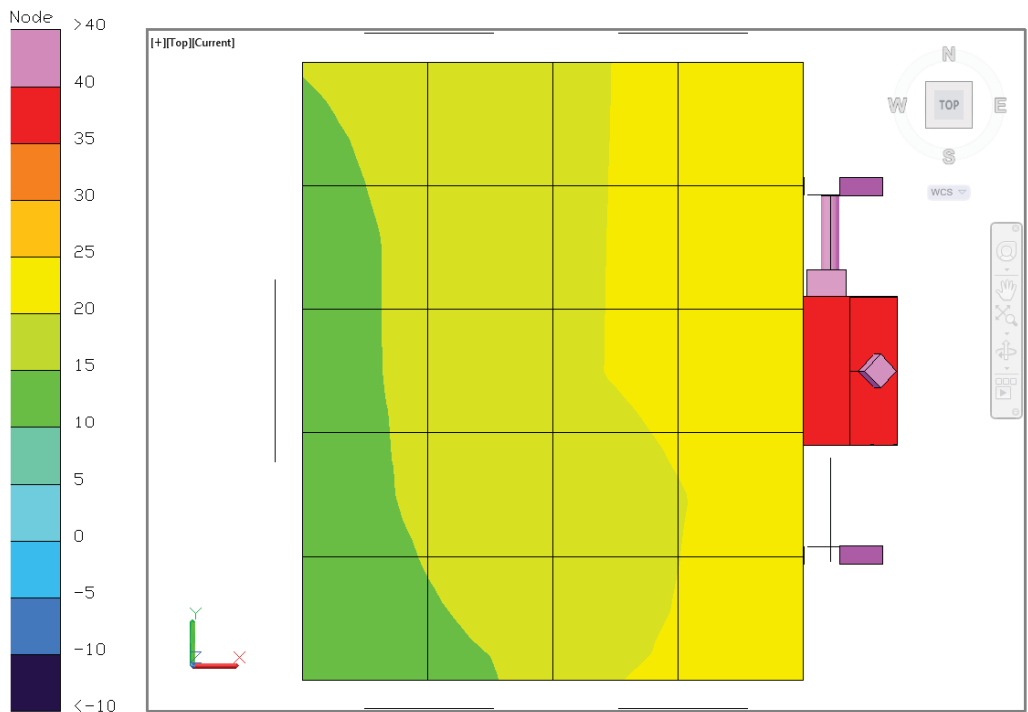**Figure 8: Orbit-averaged ExPA temperature distribution (°C) for new SAGE hot survival EOTP case.**

Table 25, Table 26, and Table 27 show comparisons between the new and previous SAGE cold op science, SAGE cold survival ELC, and SAGE cold survival EOTP cases, respectively.

Table 25: Comparison of New and Previous SAGE Cold Op Sci Cases

	Limits (°C)	New Cold Op Sci	Previous Cold Op Sci	Change
Orbital Elements (°)				
Beta		-58.9	-60.0	
Yaw		-8.4	-9.0	
Pitch		-2.0	-2.0	
Roll		0.6	0.5	
Temperatures (°C)				
Elevation Motor	-30	22.2	22.7	-0.4
Scan Mirror	-30	19.5	19.5	0.0
Attenuator	-30	21.3	21.4	-0.1
RVDT	-30	24.5	24.9	-0.4
Azimuth Motor Stator	-30	20.3	20.3	0.0
CCD	-30	6.0	6.0	0.0
CCD Controller PWA	-30	25.0	24.9	0.0
HMA	-40	5.2	5.2	0.0
HEU	-20	16.4	16.9	-0.5
ICE	-30	11.7	12.2	-0.5
IAM	-40	0.3	0.9	-0.6
CMP1	-55	-2.2	-1.8	-0.5
CMP2	-55	-4.9	-4.6	-0.3
DMP	-30	-0.7	-0.1	-0.6
Heater Duty Cycles (%)				
Scan Mirror Heater		100	100	0
SA Zone 1 Heater		46	52	-6
SA Zone 3 Heater		15	21	-6
HMA AC Heater		25	25	0
HMA UP Heater		1	1	0
CMP2 Op Heater		100	100	0

Table 26: Comparison of New and Previous SAGE Cold Survival ELC Cases

	Limits (°C)	New Cold Survival ELC	Previous Cold Survival ELC	Change
Orbital Elements (°)				
Beta		-58.9	-75.0	
Yaw		-8.4	-3.0	
Pitch		-2.0	-7.0	
Roll		0.6	0.5	
Temperatures (°C)				
Elevation Motor	-50	-10.2	-8.0	-2.2
Scan Mirror	-50	-11.2	-9.2	-2.0
Attenuator	-40	-2.0	-0.4	-1.6
RVDT	-30	-10.4	-8.1	-2.3
Azimuth Motor Stator	-30	19.3	19.4	-0.1
CCD	-30	18.6	18.7	-0.1
CCD Controller PWA	-30	17.3	17.4	-0.1
HMA	-40	4.4	5.1	-0.7
HEU	-40	-6.0	-2.3	-3.7
ICE	-30	-7.8	-7.9	0.1
IAM	-55	-23.0	-21.9	-1.1
CMP1	-55	-24.1	-23.0	-1.2
CMP2	-55	-24.4	-22.3	-2.2
DMP	-40	-15.8	-13.5	-2.3
Heater Duty Cycles (%)				
SA Zone 1 Heater		77	71	6
SA Zone 3 Heater		42	39	3
HMA AC Heater		100	100	0
HMA UP Heater		13	10	3
HEU Heater		100	100	0
ICE Survival Heater		77	70	7
IAM Survival Heater		99	0	99
DMP Survival Heater		100	100	0

Table 27: Comparison of New and Previous SAGE Cold Survival EOTP Cases

	Limits (°C)	New Cold Survival EOTP	Previous Cold Survival EOTP	Change
Orbital Elements (°)				
Beta		-3.3	10.0	
Yaw		-5.8	-6.0	
Pitch		-12.0	-12.0	
Roll		0.5	0.5	
Temperatures (°C)				
Elevation Motor	-50	**-12.6**	**-3.8**	**-8.8**
Scan Mirror	-50	**-13.0**	**-4.4**	**-8.6**
Attenuator	-40	**-3.7**	**2.5**	**-6.2**
RVDT	-30	**-12.8**	**-4.0**	**-8.8**
Azimuth Motor Stator	-30	19.2	19.5	-0.2
CCD	-30	18.3	18.4	-0.1
CCD Controller PWA	-30	17.2	17.4	-0.2
HMA	-40	4.4	5.5	-1.1
HEU	-40	-12.6	-10.2	-2.3
ICE	-30	-8.3	-7.9	-0.4
IAM	-55	-23.0	-19.7	-3.3
CMP1	-55	-25.8	-22.6	-3.2
CMP2	-55	-24.8	-20.6	-4.3
DMP	-40	-14.4	-11.4	-2.9
Heater Duty Cycles (%)				
SA Zone 1 Heater		85	80	5
SA Zone 3 Heater		47	42	5
HMA AC Heater		100	100	0
HMA UP Heater		19	13	6
HEU Heater		100	100	0
ICE Survival Heater		100	93	7
IAM Survival Heater		80	0	80
DMP Survival Heater		100	99	1

Table 28 shows a comparison of the new and previous orbits for the ISS extreme hot survival ELC case. The large temperature changes for components that are strongly conductively linked to ExPA are caused by the differences between the previous ExPA temperature distribution shown in Figure 9 and the new ExPA temperature distribution shown in Figure 10.

Table 28: Comparison of New and Previous ISS Extreme Hot Survival ELC Cases

|	Limits (°C)	New			Previous	Change
		Hot Survival ELC	Hot Survival ELC (HEU)	Hot Survival ELC (ICE)	Hot Survival ELC	
Orbital Elements (°)						
Beta		75.0	75.0	-75.0	-75.0	
Yaw		-15.0	-15.0	15.0	-7.0	
Pitch		-20.0	15.0	-20.0	-20.0	
Roll		15.0	15.0	-15.0	-15.0	
Temperatures (°C)						
Elevation Motor	85	7.2	6.0	1.7	3.6	3.6
Scan Mirror	85	6.1	5.0	-0.1	2.7	3.5
Attenuator	60	10.8	9.6	6.4	7.9	2.9
RVDT	125	7.0	5.9	1.6	3.4	3.6
Azimuth Motor Stator	65	21.4	20.1	20.0	20.0	1.3
CCD	65	21.0	19.5	19.2	19.4	1.6
CCD Controller PWA	65	22.3	19.0	20.8	18.6	3.7
HMA	80	**26.4**	15.5	25.8	**15.0**	**11.4**
HEU	80	18.7	25.3	15.7	21.4	3.9
ICE	65	10.5	4.3	**15.4**	**2.4**	**13.0**
IAM	113	**27.0**	14.1	22.2	**4.5**	**22.5**
CMP1	113	**22.4**	13.2	17.0	**4.9**	**17.5**
CMP2	113	28.2	4.3	**30.2**	**1.0**	**29.1**
DMP	75	**30.1**	9.0	29.8	**2.7**	**27.4**
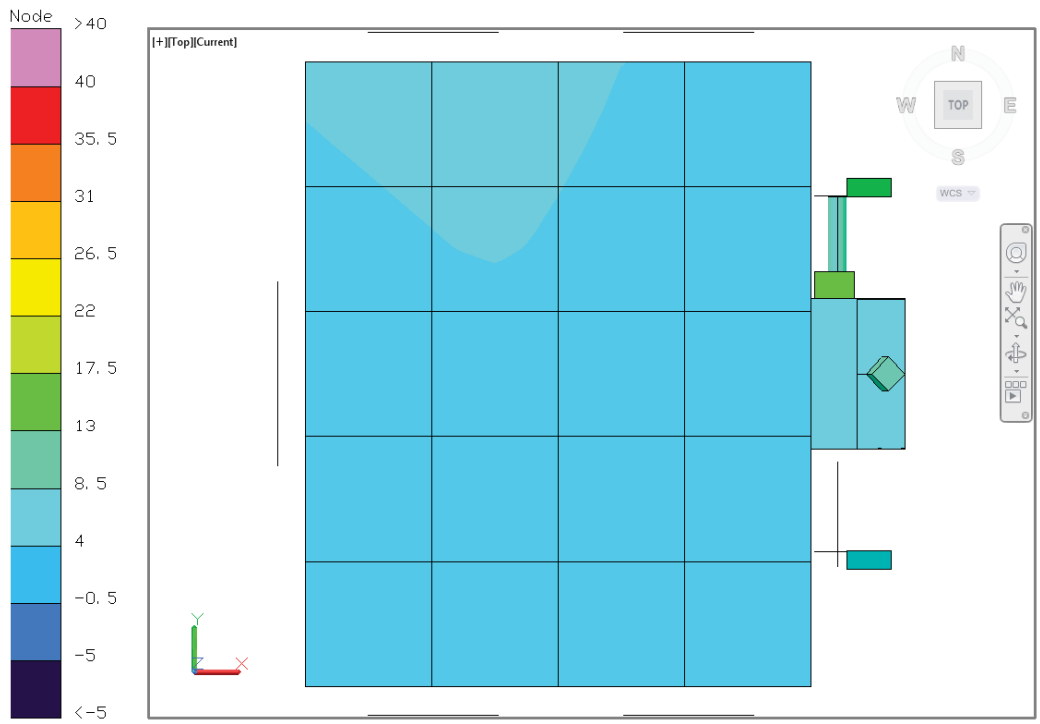
Figure 9: Orbit-averaged ExPA temperature distribution (°C) for previous ISS extreme hot survival ELC case.
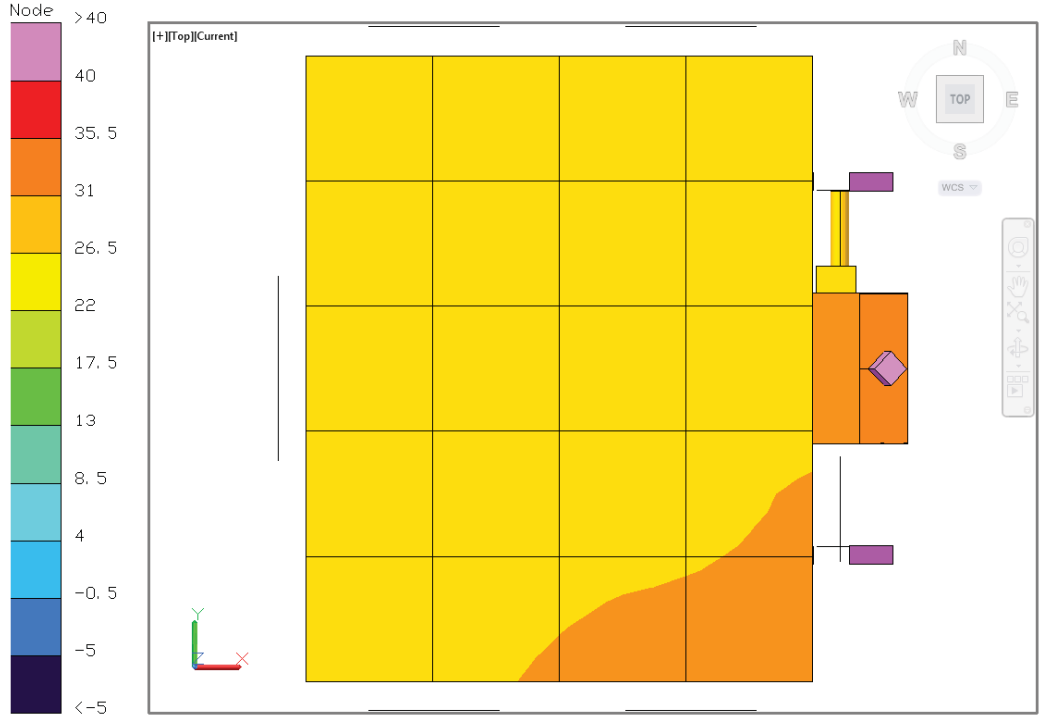

Figure 10: Orbit-averaged ExPA temperature distribution (°C) for new ISS extreme hot survival ELC case.

Table 29 shows a comparison of the new and previous orbits for the ISS extreme hot survival EOTP case. Once again, the large temperature changes for components that are strongly conductively linked to ExPA are caused by the differences between the previous ExPA temperature distribution shown in Figure 11 and the new ExPA temperature distribution shown in Figure 12. Table 30 and Table 31 show comparisons between the new and previous ISS extreme cold survival ELC and ISS extreme cold survival EOTP cases, respectively. Note that the new ISS extreme cold survival ELC case for ICE (which was the same as the previous overall ISS extreme cold survival ELC case) was removed because after including the effects of the heaters, the ICE temperature and heater duty cycle differences from the new overall cold case were no longer significant enough to warrant running an extra analysis case.

Table 29: Comparison of New and Previous ISS Extreme Hot Survival EOTP Cases

| | Limits (°C) | New | Previous | | Change |
		Hot Survival EOTP	Hot Survival EOTP	Hot Survival EOTP (IAM)	
Orbital Elements (°)					
Beta		75.0	-75.0	75.0	
Yaw		-15.0	15.0	-15.0	
Pitch		-4.1	15.0	-2.5	
Roll		-15.0	-15.0	5.0	
Temperatures (°C)					
Elevation Motor	85	**11.0**	-6.6	**3.4**	**7.6**
Scan Mirror	85	**11.3**	-6.9	**3.5**	**7.8**
Attenuator	60	**13.4**	0.5	**7.8**	**5.6**
RVDT	125	**10.8**	-6.9	**3.1**	**7.7**
Azimuth Motor Stator	65	20.2	19.5	19.9	0.4
CCD	65	19.1	18.6	18.8	0.3
CCD Controller PWA	65	21.5	18.6	19.3	2.2
HMA	80	**30.5**	15.1	**16.8**	**13.7**
HEU	80	**27.1**	12.7	**14.1**	**13.0**
ICE	65	**13.4**	-1.5	**0.3**	**13.1**
IAM	113	**35.8**	1.6	**19.0**	**16.8**
CMP1	113	**30.7**	-1.6	**15.8**	**14.9**
CMP2	113	**28.3**	-3.8	**10.0**	**18.3**
DMP	75	**35.3**	3.4	**16.8**	**18.5**
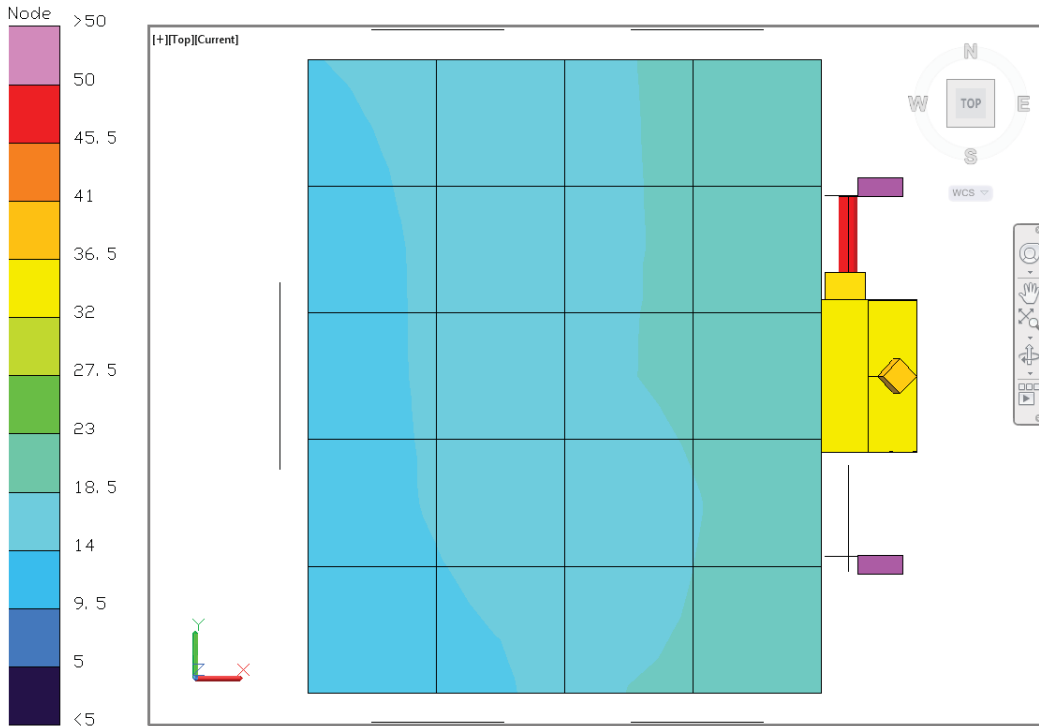
Figure 11: Orbit-averaged ExPA temperature distribution (°C) for previous ISS extreme hot survival EOTP (IAM) case.
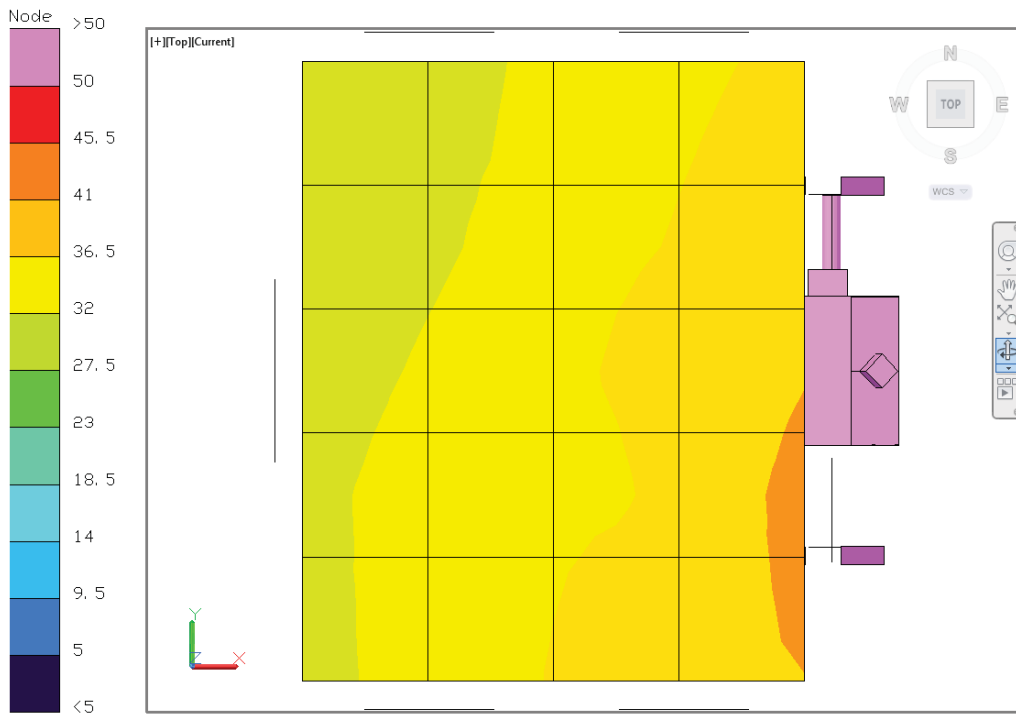

Figure 12: Orbit-averaged ExPA temperature distribution (°C) for new ISS extreme hot survival EOTP case.

Table 30: Comparison of New and Previous ISS Extreme Cold Survival ELC Cases

	Limits (°C)	New Cold Survival ELC	Previous Cold Survival ELC	Change
Orbital Elements (°)				
Beta		-75.0	-75.0	
Yaw		-15.0	15.0	
Pitch		15.0	-20.0	
Roll		13.9	15.0	
Temperatures (°C)				
Elevation Motor	-50	-14.5	-11.0	-3.4
Scan Mirror	-50	-15.7	-11.4	-4.2
Attenuator	-40	-5.1	-2.6	-2.5
RVDT	-30	-14.7	-11.3	-3.4
Azimuth Motor Stator	-30	19.2	19.3	-0.1
CCD	-30	18.4	18.4	0.0
CCD Controller PWA	-30	17.1	17.1	-0.1
HMA	-40	2.9	3.6	-0.6
HEU	-40	-14.7	-13.5	-1.2
ICE	-30	-8.0	-8.3	0.3
IAM	-55	-28.9	-25.0	-3.8
CMP1	-55	-28.1	-26.3	-1.8
CMP2	-55	-27.9	-28.3	0.0
DMP	-40	-16.8	-15.9	-0.9
Heater Duty Cycles (%)				
SA Zone 1 Heater		86	83	3
SA Zone 3 Heater		47	45	2
HMA AC Heater		100	100	0
HMA UP Heater		23	18	5
HEU Heater		100	100	0
ICE Survival Heater		99	100	-1
IAM Survival Heater		100	100	0
CMP1 Survival Heater		100	0	100
CMP2 Survival Heater		98	95	3
DMP Survival Heater		100	100	0

Table 31: Comparison of New and Previous ISS Extreme Cold Survival EOTP Cases

	Limits (°C)	New		Previous	Change
		Cold Survival EOTP	Cold Survival EOTP (CMP2, DMP, HEU & ICE)	Cold Survival EOTP	
Orbital Elements (°)					
Beta		-4.3	75.0	75.0	
Yaw		-7.0	15.0	7.0	
Pitch		-3.3	15.0	-2.5	
Roll		15.0	-8.7	-15.0	
Temperatures (°C)					
Elevation Motor	-50	-14.3	-9.1	-10.8	-3.5
Scan Mirror	-50	-14.8	-8.8	-10.5	-4.3
Attenuator	-40	-4.9	-1.2	-2.4	-2.5
RVDT	-30	-14.5	-9.3	-11.0	-3.5
Azimuth Motor Stator	-30	19.2	19.3	19.3	-0.1
CCD	-30	18.3	18.4	18.3	0.0
CCD Controller PWA	-30	17.1	17.0	17.2	-0.2
HMA	-40	3.6	2.9	4.0	-1.1
HEU	-40	-16.1	-18.9	-15.4	-3.5
ICE	-30	-8.8	-11.2	-9.5	-1.6
IAM	-55	-24.7	-25.4	-23.0	-2.4
CMP1	-55	-27.4	-27.2	-25.2	-2.2
CMP2	-55	-26.6	-28.3	-26.0	-2.2
DMP	-40	-16.6	-18.7	-15.3	-3.4
Heater Duty Cycles (%)					
SA Zone 1 Heater		89	89	88	1
SA Zone 3 Heater		48	45	47	2
HMA AC Heater		100	100	100	0
HMA UP Heater		26	30	22	8
HEU Heater		100	100	100	0
ICE Survival Heater		100	100	100	0
IAM Survival Heater		100	100	78	22
CMP1 Survival Heater		0	0	0	0
CMP2 Survival Heater		0	95	0	95
DMP Survival Heater		100	100	100	0

6   Conclusions

Revised worst-case environments were defined for both SAGE Mission Success and ISS Extreme cases on ELC-4 and EOTP using the EGO method. No special cases were required for SAGE Mission Success cases. This is desirable since those cases are run much more frequently than the ISS Extreme cases.

By comparison, the new orbits were all more extreme than the previously used orbits. These differences were fairly minor for cold cases, but more significant for most hot cases. However, these changes did not cause temperature limits to be broken for any components.

The EGO method provided additional confidence and identified slightly more extreme orbits than the orbits that would have been identified using the previous approach (simply selecting the most extreme runs from the initial DoE runs). The EGO method generally worked well, however, as with any optimization approach, the efficiency of convergence for the EGO method varies depending on the behavior of the objective function. For the severely multi-modal behavior of the EOTP cold ISS Extreme runs, the EGO method likely did not perform much better than a DoE with the same number of total runs. However, it was not known in advance which sets would be the most difficult. Thus a benefit of using an EGO approach is that it can identify which sets require the most runs.

In the future, the size of the initial DoE could be decreased. A rule of thumb for a space-filling DoE matrix when used along with an EGO algorithm is 10 runs per dimension[2], which would result in approximately 40 runs for the SAGE III environments, compared to 64 or 79 runs for this study and 69 runs for the previous study. The EGO algorithm would then be used to conduct the number of additional runs required to achieve the desired level of accuracy, likely resulting in computational savings from fewer total analysis runs.

The modification to the EGO method which allowed several of the largest local maxima to be returned at each iteration (as opposed to only the global maximum) was found to make the method much more user friendly because it reduced the total number of iterations in which the user was required to read the test points suggested by the optimizer code and start the analysis runs in the Thermal Desktop model. This modification is highly recommended for similar cases in which the optimizer code is non-integrated with the model, or to allow several test points to be run in parallel.

References

[1]   Liles, K., Amundsen, R., Davis, W., Scola, S., Tobin, S., McLeod, S., Mannu, S., Guglielmo, C., and Moeller, T. "Development and Implementation of Efficiency-Improving Analysis Methods for the SAGE III on ISS Thermal Model." Thermal & Fluid Analysis Workshop (TFAWS 13), July 29-August 2, 2013.

[2]   Jones, D., Schonlau, M., and Welch, W. 1998. "Efficient Global Optimization of Expensive Black-Box Functions." J. of Global Optimization 13, 4 (December 1998), 455-492.

[3]   Panczak, T., Ring, S., Welch, M., Johnson, D., Cullimore, B., and Bell, D. 2012. CRTech Thermal Desktop® User's Manual, v5.5

[4]   SAS Institute Inc. 2012. *Using JMP 10*. Cary, NC: SAS Institute Inc.

[5]   http://www.mathworks.com/help/optim/ug/fmincon.html

REPORT DOCUMENTATION PAGE

Form Approved
OMB No. 0704-0188

1. REPORT DATE *(DD-MM-YYYY)*	2. REPORT TYPE	3. DATES COVERED *(From - To)*
01-03-2014	Technical Memorandum	

4. TITLE AND SUBTITLE	5a. CONTRACT NUMBER

Selection of Thermal Worst-Case Orbits via Modified Efficient Global Optimization

5b. GRANT NUMBER

5c. PROGRAM ELEMENT NUMBER

6. AUTHOR(S)	5d. PROJECT NUMBER

Moeller, Timothy M.; Wilhite, Alan W.; Liles, Kaitlin A.

5e. TASK NUMBER

5f. WORK UNIT NUMBER
857865.02.01

7. PERFORMING ORGANIZATION NAME(S) AND ADDRESS(ES)	8. PERFORMING ORGANIZATION REPORT NUMBER
NASA Langley Research Center Hampton, VA 23681-2199	L-20365

9. SPONSORING/MONITORING AGENCY NAME(S) AND ADDRESS(ES)	10. SPONSOR/MONITOR'S ACRONYM(S)
National Aeronautics and Space Administration Washington, DC 20546-0001	NASA
	11. SPONSOR/MONITOR'S REPORT NUMBER(S) NASA/TM-2014-218182

12. DISTRIBUTION/AVAILABILITY STATEMENT
Unclassified - Unlimited
Subject Category 31
Availability: NASA CASI (443) 757-5802

13. SUPPLEMENTARY NOTES

14. ABSTRACT

Efficient Global Optimization (EGO) was used to select orbits with worst-case hot and cold thermal environments for the Stratospheric Aerosol and Gas Experiment (SAGE) III. The SAGE III system thermal model changed substantially since the previous selection of worst-case orbits (which did not use the EGO method), so the selections were revised to ensure the worst cases are being captured. The EGO method consists of first conducting an initial set of parametric runs, generated with a space-filling Design of Experiments (DoE) method, then fitting a surrogate model to the data and searching for points of maximum Expected Improvement (EI) to conduct additional runs. The general EGO method was modified by using a multi-start optimizer to identify multiple new test points at each iteration. This modification facilitates paralell computing and decreases the burden of user interaction when the optimizer code is not integrated with the model. Thermal worst-case orbits for SAGE III were successfully identified and shown by direct comparison to be more severe than those identified in the previous selection. The EGO method is a useful tool for this application and can result in computational savings if the initial Design of Experiments (DoE) is selected appropriately.

15. SUBJECT TERMS

SAGE; optimization; thermal analysis

16. SECURITY CLASSIFICATION OF:			17. LIMITATION OF ABSTRACT	18. NUMBER OF PAGES	19a. NAME OF RESPONSIBLE PERSON
a. REPORT	b. ABSTRACT	c. THIS PAGE			STI Help Desk (email: help@sti.nasa.gov)
U	U	U	UU	44	19b. TELEPHONE NUMBER *(Include area code)* (443) 757-5802

Standard Form 298 (Rev. 8-98)
Prescribed by ANSI Std. Z39.18